

# Natural Convective Flow Inside a Confined Enclosure Filled with Hybrid Nanofluid: Finite Volume Method

*Ibtissam Hadri<sup>1\*</sup>, Anass Bendaraa<sup>1</sup>, Asmaa Wina<sup>1</sup>, and Moulay Mustapha Charafi<sup>1</sup>*

<sup>1</sup>LS2ME polydisciplinary faculty of Khouribga, Sultan Moulay Slimane University BP: 145 25000, Morocco.

**Abstract.** This work investigates heat transfer enhancement using natural convection in a square cavity filled with Cu-Ag/water (75:25) and Cu-Au/water (75:25) hybrid nanofluids. The physical model and governing equations including continuity, momentum, and energy are formulated and solved using the finite volume method (FVM). The analysis explores different conditions, including Rayleigh numbers ranging from  $10^3$  to  $10^5$ , which correspond to weak to strong convection, and nanoparticle volume fractions between 0.01 and 0.03. These parameters are studied to understand their impact on heat transfer performance. The results show that adding nanoparticles clearly improves convective heat transfer. The average Nusselt number increases as the nanoparticle concentration rises, and this effect becomes even more pronounced at higher Rayleigh numbers due to stronger buoyancy-driven flow. It is also observed that the Cu-Ag hybrid nanofluid performs slightly better than the Cu-Au one. Overall, these findings suggest that hybrid nanofluids can be an effective solution for enhancing natural convection, with potential applications in areas such as electronics cooling, solar energy systems, and heat exchangers.

**Keywords:** Natural Convection, hybrid Nanofluid, Finite Volume Method, Rayleigh

## Nomenclature

### Latin symbols

$g$  gravitational acceleration ( $\text{m}\cdot\text{s}^{-2}$ )  
 $L$  characteristic length of the cavity (m)  
 $k$  thermal conductivity ( $\text{W}\cdot\text{m}^{-1}\cdot\text{K}^{-1}$ )  
 $Nu$  Nusselt number  
 $p$  pressure (Pa)  
 $Pr$  Prandtl number  
 $Ra$  Rayleigh number  
 $T$  temperature (K)  
 $u, v$  velocity components in x and y directions ( $\text{m}\cdot\text{s}^{-1}$ )  
 $x, y$  Cartesian coordinates (m)

### Greek symbols

---

\* Corresponding author: [ibtissamhadri2@gmail.com](mailto:ibtissamhadri2@gmail.com)

- $\alpha$  thermal diffusivity ( $\text{m}^2 \cdot \text{s}^{-1}$ )
- $\beta$  thermal expansion coefficient ( $\text{K}^{-1}$ )
- $\phi$  volume fraction (%)
- $\mu$  dynamic viscosity ( $\text{Pa} \cdot \text{s}$ )
- $\nu$  kinematic viscosity ( $\text{m}^2 \cdot \text{s}^{-1}$ )
- $\rho$  density ( $\text{kg} \cdot \text{m}^{-3}$ )
- $\theta$  dimensionless temperature.

#### **Subscripts and Superscripts**

- Cu Copper nanoparticles ;
- Ag Silver nanoparticles ;
- Au Gold nanoparticles ;
- Avg Average value;
- $f$  base fluid (water)
- np nanoparticle
- hnf hybrid nanofluid
- hp hybrid nanoparticle
- $c$  cold wall
- $h$  hot wall

## **1 Introduction**

Natural convection, also called free convection, is a fluid flow mechanism driven by density variations induced by temperature differences. Warmer fluid regions become less dense and rise under the effect of gravity, while cooler and denser regions move downward. This buoyancy-induced motion results in the formation of convective currents within the fluid[1]. The study of natural convection in cavities filled with hybrid nanofluids has received considerable attention in recent years. This interest is mainly attributed to the strong influence of cavity geometry and boundary conditions on flow behaviors; the thermophysical properties of hybrid nanofluids play a crucial role in the enhancement of heat transfer performance. A. Bendaraa et al [2]demonstrated that increasing the nanoparticle concentration enhances heat transfer in a heat exchanger, with optimal performance achieved using the  $\text{Al}_2\text{O}_3/\text{Cu}$  hybrid mixture. In the context of natural convection in different cavities, several studies have highlighted the combined role of hybrid nanofluids and the Rayleigh number ; in a square cavity W. Amlal et al. [3][4] showed that, in the context of natural convection under a magnetic field, the addition of nanoparticles and an increase in the Reynolds number enhance heat transfer, whereas the magnetic field and buoyancy effects can reduce it. Z. Abdel-Nour et al. [5] showed that magnetic field orientation influences entropy generation and flow symmetry in a square porous cavity filled with hybrid nanofluid. In a trapezoidal cavity; M. Hashim et al. [6] showed that the interaction between the nanoparticle volume fraction and the Rayleigh number significantly enhances heat transfer. Similarly, in a triangular cavity; Md. Rakibul Hasan et al. [7] showed that increasing the Rayleigh number modifies vortex structure and enhances heat transfer in triangular cavities with sinusoidal heating. S. Khalatbari et al.[8] indicated that increasing the Rayleigh number strengthens convective motions and improves the overall heat transfer rate with an internal cooled circular cylinder. And Y. Turabi et al. [9] showed that wall geometry and magnetic field inclination control vortex structure and entropy generation in a wavy triangular cavity with a cold cylinder. In a complex cavity; H. R. Ashorynejad et al. [10] showed that the application of a magnetic field suppresses flow intensity and promotes a more uniform temperature distribution in an open wavy cavity filled with hybrid nanofluid. Ghalambaz et al. [11] showed that the use of a hybrid nanofluid in a complex-shaped

cavity promotes the formation of multiple vortices and enhances temperature distribution.

Most previous studies examined only one type of hybrid nanofluid, making direct comparison difficult. This study compares Cu–Ag/water (75:25) and Cu–Au/water (75:25) hybrid nanofluids under the same conditions. The same boundary conditions and nanoparticle concentrations are used for both cases. The finite volume method (FVM) is applied to solve the governing equations accurately.

This study examines two main parameters; First, the Rayleigh number (Ra) is varied from  $10^3$  to  $10^5$  to study weak and strong convection. Second, the nanoparticle volume fraction ( $\phi$ ) is changed from 1% to 3% to see its effect on heat transfer. The nanofluid is assumed to be Newtonian, incompressible, and homogeneous. Its properties are constant, and thermal equilibrium is considered. The Boussinesq approximation is used for density variation. Viscous dissipation and heat generation are neglected. These assumptions simplify the model and allow accurate numerical simulation.

This study investigates the effects of the Rayleigh number and nanoparticle volume fraction on natural convection. It analyzes their influence on temperature distribution, flow structure, and heat transfer inside the cavity. A comparison between Cu–Ag and Cu–Au hybrid nanofluids is also carried out to evaluate the effect of different metallic nanoparticles on thermal performance.

## 2 Mathematical Formulation

### 1.1 The geometrical configuration of the square cavity

A square cavity of side length (L), filled with a hybrid nanofluid (Cu–Ag/water or Cu–Au/water), defined in a two-dimensional Cartesian coordinate system ((x, y)). bounded by four rigid walls; The left vertical wall is maintained at a uniform hot temperature  $T_h$ , while the right vertical wall is kept at a constant cold temperature  $T_c$ . The top and bottom horizontal walls are adiabatic, these thermal boundary conditions are expressed as:

$$\begin{aligned} T &= T_h & \text{at } x=0, 0 \leq y \leq L; \\ T &= T_c & \text{at } x=L, 0 \leq y \leq L; \\ \partial T / \partial y &= 0 & \text{at } y=0 ; y=L, 0 < y < L; \end{aligned}$$

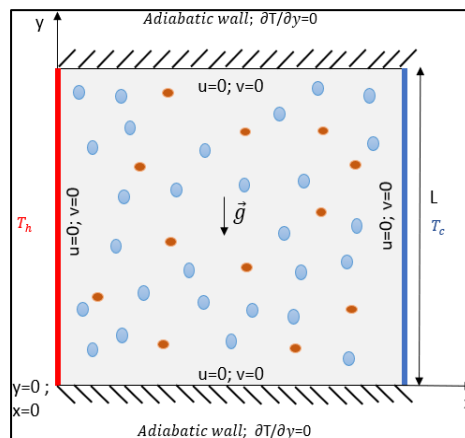


**Fig. 1.** The studied configuration consists of a square cavity filled with a hybrid nanofluid.

All cavity walls are assumed to be impermeable and stationary, imposing a no-slip condition on the fluid velocity:

$$u=v=0 \quad \text{on all walls.}$$

The geometrical configuration of the square cavity with the boundary conditions associated with the dimensional and dimensionless analysis (Fig 1).

### 1.2 Governing equations

The flow is assumed two-dimensional, laminar, incompressible. Thermophysical properties are considered constant except for the density variation in the buoyancy term, modelled using the Boussinesq approximation.

Using the dimensionless groups as follow:

$$X= x/L ; \quad Y= y/L ; \quad U= u L/\alpha_f ; \quad V= v L/\alpha_f ; \quad P=(p L^2)/(\rho_{hnf} \alpha_f^2) ; \\ \theta=(T-T_c)/(T_h-T_c) ;$$

The dimensionless governing equations are expressed as follows (Eqs. 1-4):

**Equation of continuity:**

$$\partial U/\partial X+\partial V/\partial Y=0 \tag{1}$$

**Navier-Stokes Equations:**

**Along x**

$$\partial U/\partial t+U^* \partial U/\partial X+V^* \partial U/\partial Y=-\partial P/\partial X+[(\mu_{hnf}/(\rho_{hnf} \alpha_f)) * ((\partial^2 U)/(\partial X)^2 + (\partial^2 U)/(\partial Y)^2)] \tag{2}$$

**Along y**

$$\partial V/\partial t+U^* \partial V/\partial X+V^* \partial V/\partial Y=-\partial P/\partial Y+ [(\mu_{hnf}/(\rho_{hnf} \alpha_f)) * ((\partial^2 V)/(\partial X)^2 + (\partial^2 V)/(\partial Y)^2)] + ((\rho\beta)_{hnf}/(\rho_f \beta_f)) * Ra.Pr.\theta \tag{3}$$

**Energy Equation :**

$$\partial \theta/\partial t+U^* \partial \theta/\partial X+V^* \partial \theta/\partial Y= [(\alpha_{hnf}/(\alpha_f)) * ((\partial^2 \theta)/(\partial X)^2 + (\partial^2 \theta)/(\partial Y)^2)] \tag{4}$$

With

$$\alpha_{hnf}=k_{hnf}/(\rho_{hnf} * (Cp)_{hnf}) ; \quad Ra_{hnf}=(g \beta_{hnf} \rho_{hnf} .\Delta T.L^3)/(\mu_{hnf} \alpha_{hnf}) \quad ; \quad Pr_{hnf}=\mu_{hnf}/(\rho_{hnf} \alpha_{hnf}) ;$$

In the case of hybrids nanofluids, the local Nusselt number will depend on the ratio of thermal conductivities.

$$Nu= (-k_{hnf}/k_f) \partial \theta/\partial X|_{(X=0)} \tag{5}$$

The average Nusselt number is defined as:

$$Nu_{avg}=\int Nu(X).dX \tag{6}$$

### 1.3 hybrid nanofluids properties

For a given total nanoparticle volume fraction  $\phi$ , the hybrid composition 75:25 refers to the volume fraction split between the two nanoparticles, such that:

$$\phi_{np1}= 0.75 \phi; \quad \phi_{np2}=0.25 \phi \tag{7}$$

$$\rho_{hp}= ((\phi_{np1} \rho_{np1} + \phi_{np2} \rho_{np2})) / \phi_{hp} \tag{8}$$

$$(Cp)_{hp}=(\phi_{np1}(Cp)_{np1} + \phi_{np2}(Cp)_{np2})/ \phi_{hp} \tag{9}$$

$$k_{hp} = ((\varphi_{np1} k_{np1} + \varphi_{np2} k_{np2})) / \varphi_{hp} \tag{10}$$

$$\beta_{hp} = ((\varphi_{np1} \beta_{np1} + \varphi_{np2} \beta_{np2})) / \varphi_{hp} \tag{11}$$

The properties of the hybrid nanofluid, namely the hybrid nanoparticle volume fraction ( $\varphi_{hnf}$ ), density ( $\rho_{hnf}$ ), heat capacity ( $(Cp)_{hnf}$ ), thermal conductivity ( $k_{hnf}$ ), and viscosity ( $\mu_{hnf}$ ) are defined as follows:

For the conductivity using the Maxwell Model:

$$k_{hnf} = k_f [(K_{hp} + 2k_f + 2(k_{hp} - k_f) * \varphi_{hp}) / (k_{hp} + 2k_f + (k_f - k_{hp}) * \varphi_{hp})] \tag{12}$$

The specific heat of the hybrid nanofluid is calculated from Pak & Cho model:

$$(Cp)_{hnf} = \varphi_{hp} (Cp)_{hp} + (1 - \varphi_{hp})(Cp)_f \tag{13}$$

For the viscosity using the Einstein model:

$$\mu_{hnf} = \mu_f (1 + 2.5 * \varphi_{hp}) \tag{14}$$

The Einstein viscosity and Maxwell thermal conductivity models are theoretically derived for very dilute suspensions ( $\varphi < 2-5$ ), they are routinely employed in recent hybrid nanofluid studies up to  $\varphi = 3$ , with reasonable agreement to experimental data[12].

For the Density

$$\rho_{hnf} = (1 - \varphi_{hp}) \rho_f + \varphi_{hp} \rho_{hp} \tag{15}$$

For the thermal expansion coefficient:

$$\beta_{hnf} = (1 - \varphi_{hp}) \beta_f + \varphi_{hp} \beta_{hp} \tag{16}$$

The parameters that characterize the natural convective heat transfer inside the square cavity are determined by several thermophysical properties of the hybrid nanofluids, including thermal conductivity, specific heat capacity, dynamic viscosity, thermal expansion coefficient, and kinematic viscosity (Table 1).

**Table 1.** Thermophysical properties of the materials used throughout this research.

Thermophysical properties	f (Water)	Cu	Au	Ag
Cp (J.kg <sup>-1</sup> .K <sup>-1</sup> )	4181.8	390	129.81	235
ρ (kg.m <sup>-3</sup> )	998,2	8930	19320	10500
k (W.m <sup>-1</sup> .K <sup>-1</sup> )	0,593	400	297.73	429
β (K <sup>-1</sup> )	2.07 *10 <sup>-4</sup>	1.67 *10 <sup>-5</sup>	1.42 *10 <sup>-5</sup>	1.89 *10 <sup>-5</sup>
μ*10 <sup>-3</sup> (kg.m <sup>-1</sup> .s <sup>-1</sup> )	1.002	-----	-----	-----

Based on the thermophysical properties of the hybrid nanofluid (Eqs. 7– 16) and the values of the base fluid and the nanoparticles used, the Prandtl number values are determined for each nanoparticle volume fraction (Table 2).

**Table 2.** Prandtl number as a function of the nanoparticle volume fraction for water-based hybrid nanofluids Cu-Ag and Cu-Au.

Volume Fraction	Pr Number	
	Cu-Ag	Cu-Au
1%	6.897	6.975
2%	6.86	6.866
3%	6.76	6.762

### 3 Numerical Method

The dimensionless governing equations (1-4) were solved using the finite volume method with a structured staggered grid, implemented in MATLAB.

A structured staggered grid was used to discretize the computational domain.

The computational domain was divided into a finite number of control volumes, as shown in Figure 2(a), within which the conservation equations are integrated. Each control volume was associated with a main node (P), at which the average values of the unknown variables (velocity, pressure, and temperature) were stored. Each node (P), The neighbouring nodes E and W correspond to the east and west directions along the x-axis, while N and S denote the north and south directions along the y-axis. The control volume is outlined by dashed lines, with faces located at points (e) and (o) along the (X)axis, and (n) and (s) along the (Y) axis as shown in Figure 2; In contrast, vector quantities such as the velocity components (u) and (v) are stored at the East and North faces of the control volumes as shown in Figure 2(b). To minimize numerical errors and avoid pressure-velocity decoupling, the momentum equations were solved in staggered control volumes. These volumes were shifted to the right for the x-direction velocity component and upward for the y-direction velocity component.

The pressure-velocity coupling was handled using the SIMPLE algorithm. The discretized momentum equations were first solved to obtain provisional velocity fields. A pressure correction equation was then derived from the continuity constraint and solved to update the pressure and velocity fields.

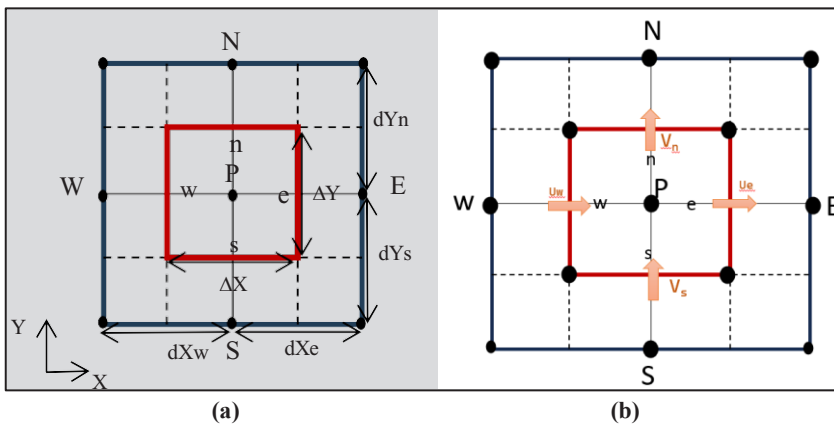


**Fig. 2.** Mesh representation schematic.

The convective terms in the governing equations were discretized using the first-order upwind scheme, while the diffusive terms were approximated using second-order central differences. Buoyancy effects were modelled using the Boussinesq approximation, in which

density variations were considered only in the buoyancy term of the vertical momentum equation.

Pressure, temperature, and velocity fields were calculated inside the control volumes.

The SIMPLE algorithm was applied for pressure–velocity coupling.

The upwind scheme was used for convective terms, while central differences were used for diffusive terms.

The convergence of the numerical calculations was ensured by iterating until the maximum relative change of each primary variable fell below  $10^{-6}$ , according to the following relation:

$$\max|(\phi^{n+1}-\phi^n)/\phi^n| < 10^{-6}, \phi=U,V,P,\theta; \tag{17}$$

**Table 3.** Comparison of the average Nusselt number with previous studies for different Ra-values (Pr=0.71,  $\phi = 0$ ).

Nu average				
	Present work	Khanafer et al.[13]	Vahl Davis et al.[14]	Boualit et al.[15]
Ra=10 <sup>3</sup>	1.1187	1.118	1.118	1.118
Ra=10 <sup>4</sup>	2.2442	2.245	2.243	2.247
Ra=10 <sup>5</sup>	4.5169	4.522	4.519	4.550
Ra=10 <sup>6</sup>	8.8174	8.826	8.799	9.185

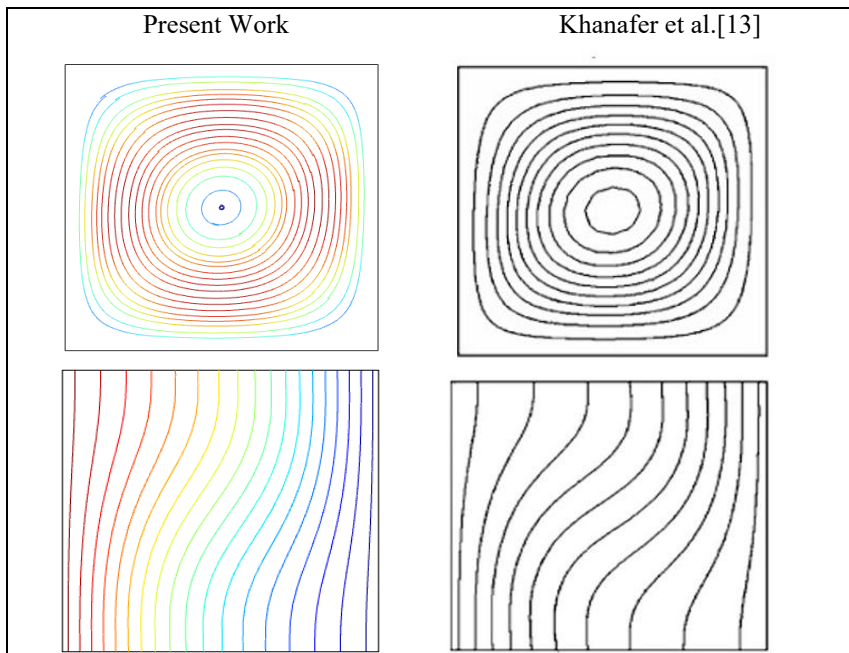


**Fig. 3.** Comparison of the streamlines and the isotherms between the present work, Khanafer et al.[13] (Pr = 0.7, Ra = 10<sup>3</sup>).

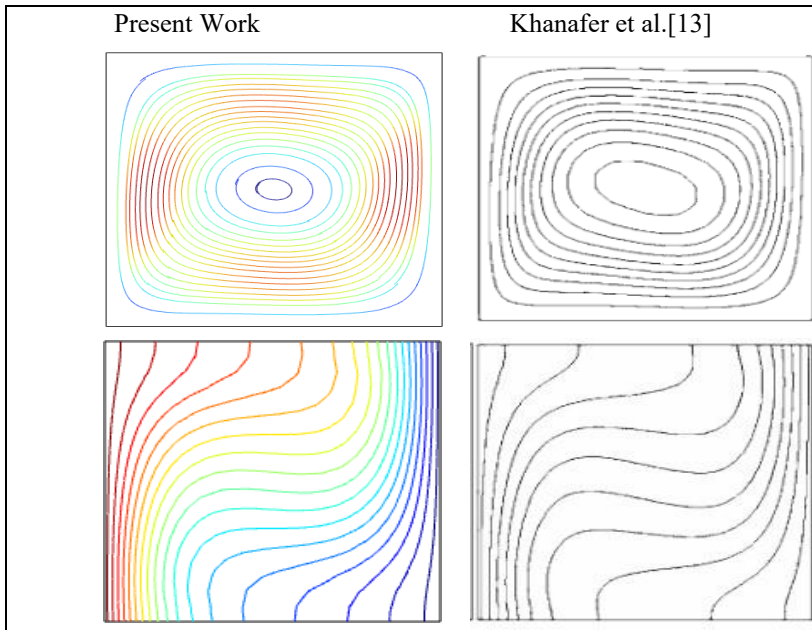


**Fig. 4.** Comparison of the streamlines and the isotherms between the present work, Khanafer et al.[13] ( $Pr = 0.7, Ra = 10^4$ ).

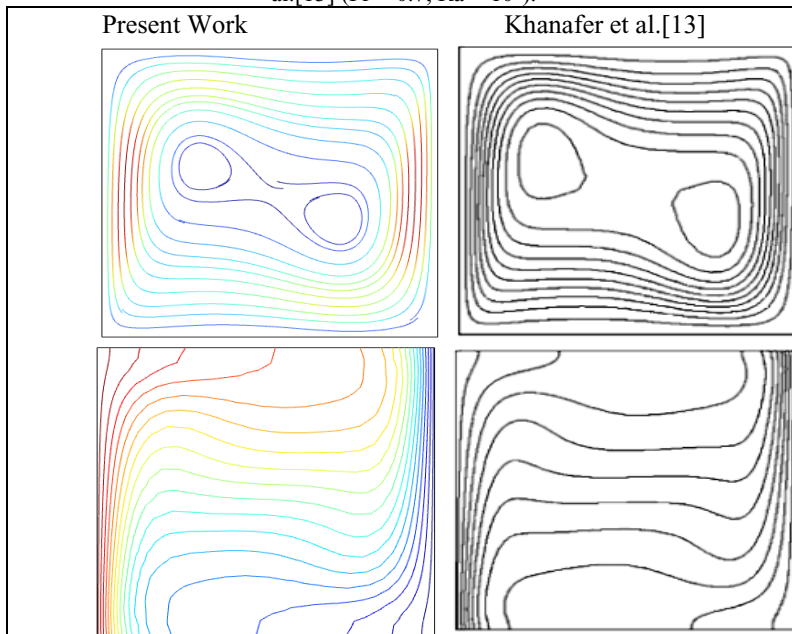


**Fig. 5.** Comparison of the streamlines and the isotherms between the present work, Khanafer et al.[13] ( $Pr = 0.7, Ra = 10^5$ ).

### 3.1 Grid testing and code validation

The numerical method was validated by comparing the average Nusselt number with results from previous studies[13]- [15] (Table 3 ). The comparison was performed for Rayleigh numbers from  $10^3$  to  $10^6$  at  $Pr = 0.71$  for a pure fluid.

The results showed excellent agreement, confirming the accuracy of the numerical model. A qualitative comparison was also performed with the results of Khanafer et al.[13]. Temperature and velocity fields were compared for a pure fluid at  $Pr = 0.71$ . The analysis was carried out for Rayleigh numbers from  $10^3$  to  $10^4$  to examine flow and thermal patterns inside the cavity.

The numerical results show good qualitative agreement with the reference data, capturing the main features of natural convection, such as the structure of streamlines and isotherms as shown in figures 3-5. This confirms that the developed code correctly reproduces the convective behaviour in a square cavity.

## 4 Results and Discussion

### 4.1 Influence of the Rayleigh number

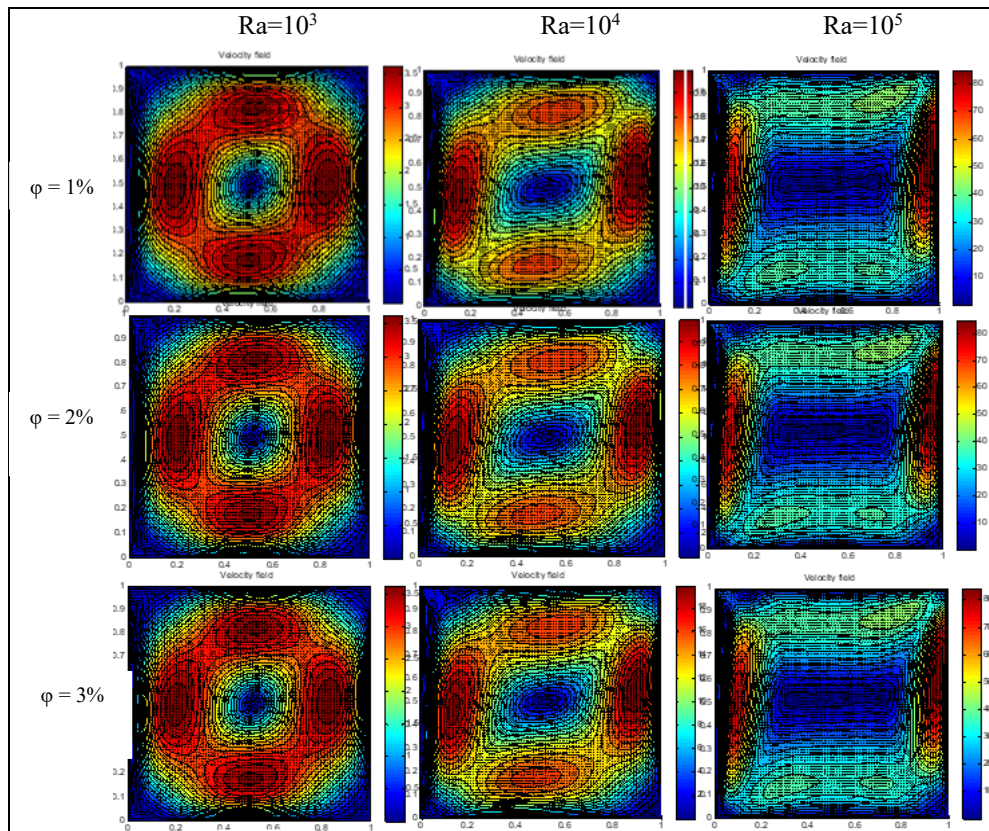


**Fig. 6.** Velocity structure for different Rayleigh numbers ( $Ra = 10^3$ - $10^5$ ) and different volume fractions (1-3%) for the water-based Cu–Ag hybrid nanofluid.

The figures 6-9 illustrating the velocity fields and temperature isotherms of the water-based Cu Ag and Cu Au hybrid nanofluids.

At  $Ra = 10^3$ , the flow is weak and heat transfer is mainly by conduction. At  $Ra = 10^4$ , vortices become larger and convection effects increase. At  $Ra = 10^5$ , strong convection cells appear

and fluid velocity increases near the walls. These results show that increasing the Rayleigh number changes the heat transfer from conduction-dominated to convection-dominated flow.

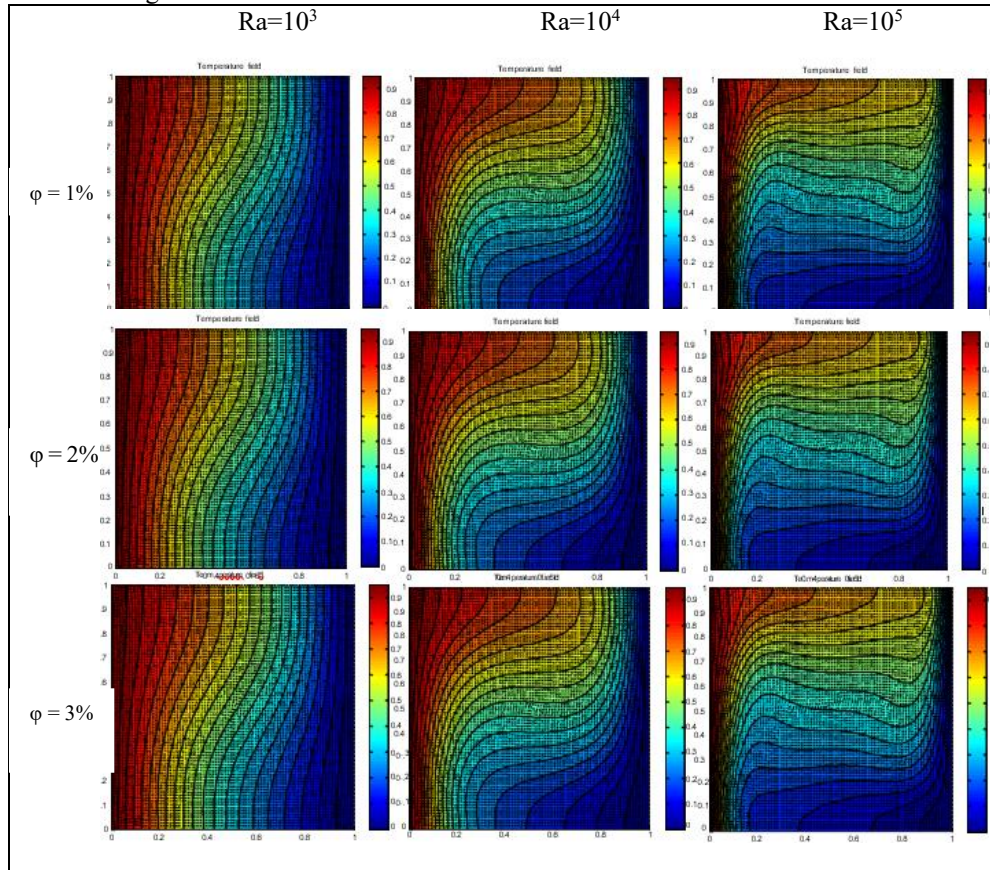


**Fig. 7.** Temperature isotherm structure for different Rayleigh numbers ( $Ra = 10^3$ - $10^5$ ), and for different volume fractions (1- 3%) for the water-based Cu–Ag hybrid nanofluid.

These observations demonstrate that  $Ra$  governs the transition from a conduction-dominated regime to fully developed natural convection.

The qualitative analysis of the flow and temperature fields shows that increasing the Rayleigh number strengthens convective motion, and modifies the thermal structures inside the cavity.

These observations are confirmed by quantitative results. Figures 10 and 12, along with Tables 5 and 6, show that the average Nusselt number increases systematically with  $Ra$ ;  $Nu$  remains low at  $Ra = 10^3$ , rises noticeably at  $Ra = 10^4$ , and reaches its maximum at  $Ra = 10^5$ , corresponding to fully developed convection. This monotonic increase demonstrates that stronger buoyancy forces enhance thermal transport efficiency within the cavity.

#### 4.2 Influence of the nanoparticle volume fraction ( $\phi$ ) on heat transfer

Increasing the nanoparticle volume fraction significantly modifies both the flow structures and the thermal distribution inside the cavity (Figures 6-9). The temperature isotherms show that when  $\phi$  increases, the temperature lines become more compressed near the hot wall, indicating a stronger thermal gradient. This compression reflects an enhancement of both

conductive and convective heat transfer. Similarly, the streamlines become more stretched and form a more energetic main vortex, which reveals a more vigorous internal circulation of the nanofluid.

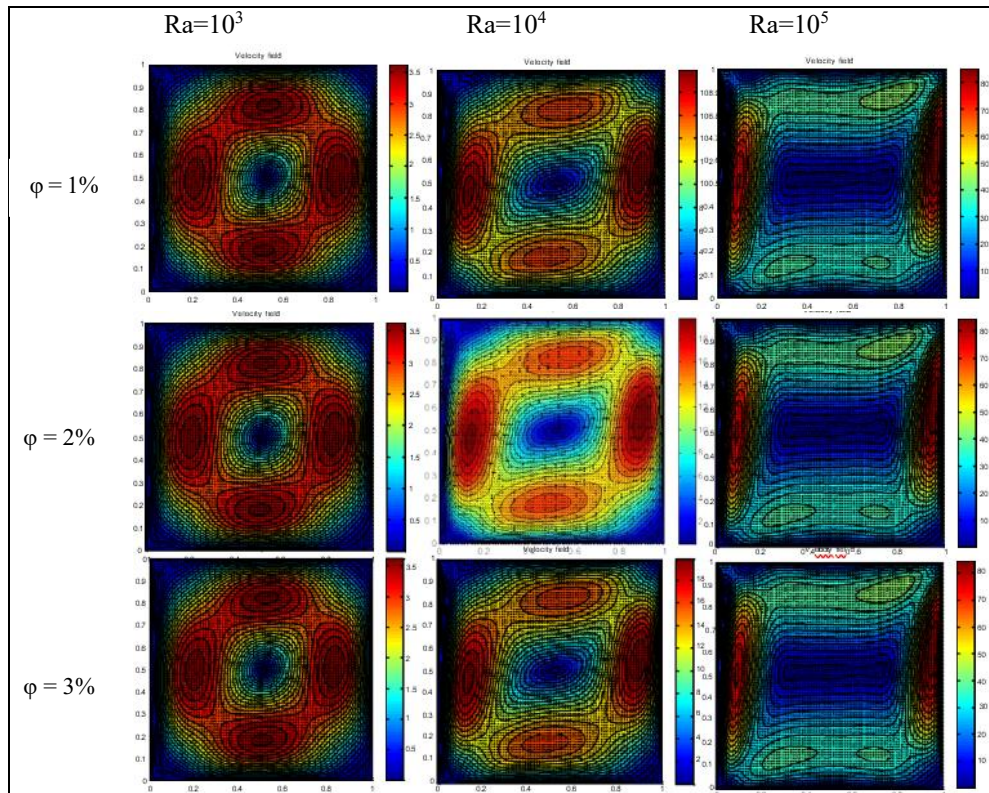


**Fig. 8.** Velocity structure for different Rayleigh numbers ( $Ra = 10^3$ - $10^5$ ) and different volume fractions (1- 3%) for the water-based Cu–Au hybrid nanofluid.

**Table 4.** Average Nusselt number as a function of Rayleigh number and of volume fraction for the water-based Cu–Ag hybrid nanofluid.

	The average Nusselt		
	1%	2%	3%
$Ra=10^3$	1.319915192	1.350474006	1.388523274
$Ra=10^4$	2.509004884	2.56726148	2.639655493
$Ra=10^5$	5.071352484	5.201908741	5.348549775

The results also show that adding nanoparticles increases the effective thermal conductivity of the base fluid, which leads to a systematic rise in the average Nusselt number. The curves of  $Nu$  as a function of  $\phi$  clearly illustrate this improvement (Figure 11), (Table 4) and (Figure 13), (Table 5): for every Rayleigh number, the Nusselt number increases with the volume

fraction, confirming that hybrid nanofluids enhance heat transfer. This effect is even more pronounced for the Cu–Ag and Cu–Au hybrids, whose superior thermal properties further strengthen natural convection.

**Table 5.** Average Nusselt number as a function of Rayleigh number and of volume fraction for the water-based Cu–Au hybrid nanofluid.

	The average Nusselt		
	1%	2%	3%
$Ra=10^3$	1.304971635	1.345572909	1.38848126
$Ra=10^4$	2.480553077	2.557796324	2.639574398
$Ra=10^5$	5.013884993	5.193655761	5.348386413

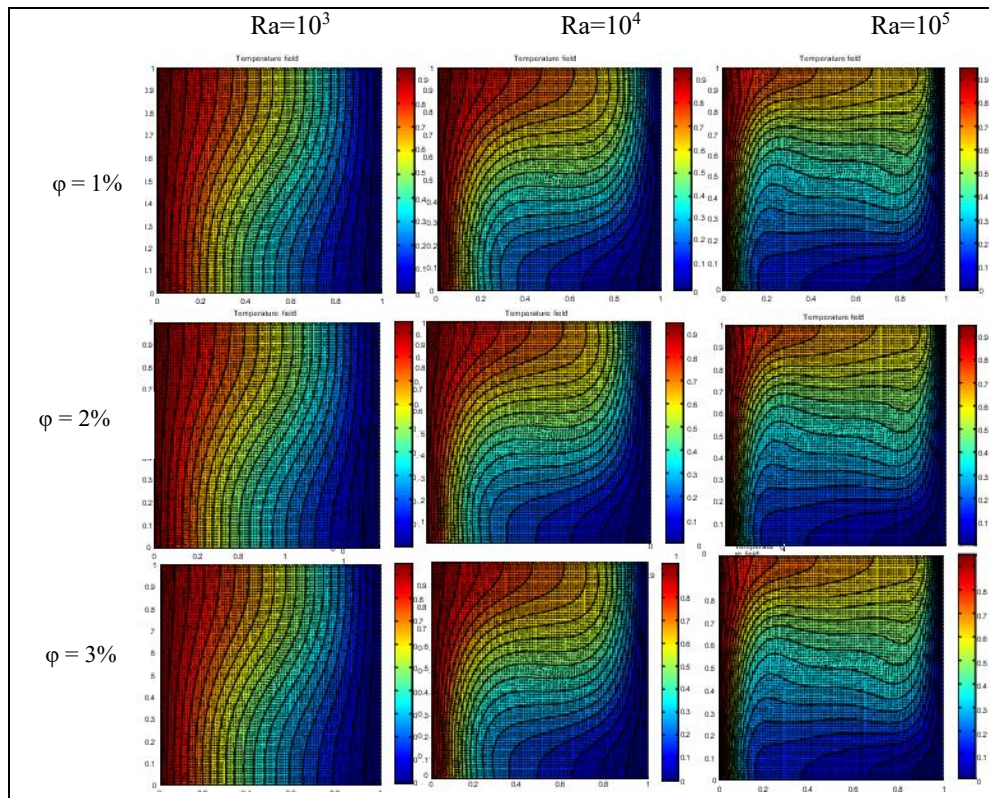


**Fig. 9.** Temperature isotherm structure for different Rayleigh numbers ( $Ra = 10^3-10^5$ ), and for different volume fractions (1- 3%) for the water-based Cu–Au hybrid nanofluid.

### 4.3 The Comparison between the two hybrids nanofluids

The hybrid nanofluids Cu-Ag and Cu-Au exhibit a clear enhancement of natural convective heat transfer compared with pure water, with average improvements of

approximately 17- 23% in the mean Nusselt number ( $Nu_{avg}$ ). While pure water typically yields values of about 1,10 2,20 and 4,30 as the Rayleigh number increases, the corresponding values for the hybrid nanofluids reach approximately 1,35; 2,57, and 5,20. The enhancement is most pronounced at  $Ra=10^3$  (around +23%), where heat transfer remains partially conduction-dominated, and remains substantial at  $Ra=10^5$  (around +21%), confirming the performance of nanoparticle addition across all convection regimes.

The comparison between the Cu-Ag and Cu-Au hybrid nanofluids indicates that the differences in thermal performance are very small across all cases considered as shown in tables 5-6. The reported average Nusselt numbers show a slight advantage for Cu-Ag over Cu-Au; however, this advantage is marginal and, in some instances, remains below the one-percent level.

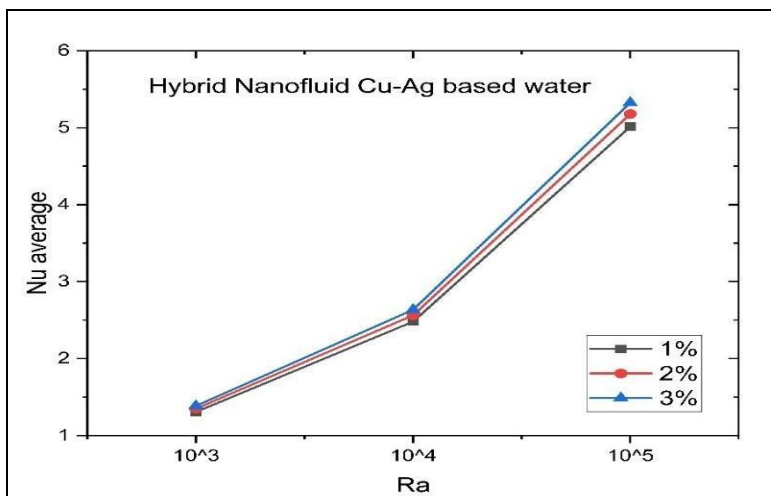


**Fig. 10.** Average Nusselt number as a function of Rayleigh number for the water-based Cu–Ag hybrid nanofluid.

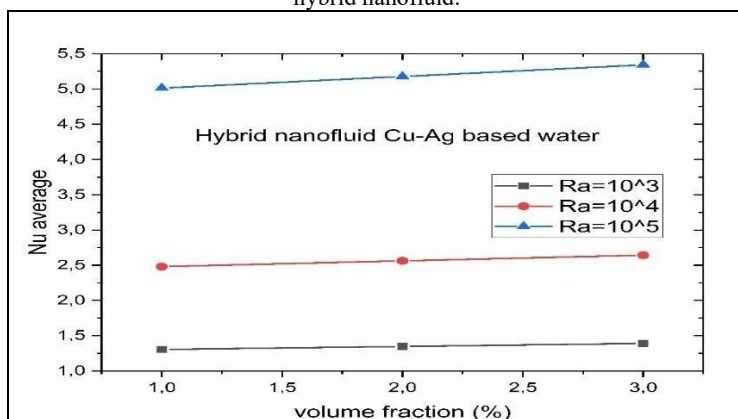


**Fig. 11.** Average Nusselt number as a function of volume fraction for the water-based Cu–Ag hybrid nanofluid.

Such minimal differences suggest that the observed discrepancies may be attributed to residual numerical uncertainties as well as to assumptions inherent in the thermophysical property models used. In particular, the limited variations in the effective thermal conductivity of silver and gold, once incorporated within a homogenized modelling framework, result in nearly identical convective behaviors.

Although Cu-Ag consistently exhibits slightly higher Nusselt numbers, this superiority cannot be considered practically significant. The results indicate that both hybrid nanofluids provide equivalent thermal performance under natural convection conditions, and the choice of the secondary metallic component is secondary compared to the dominant effects of the Rayleigh number and nanoparticle volume fraction.

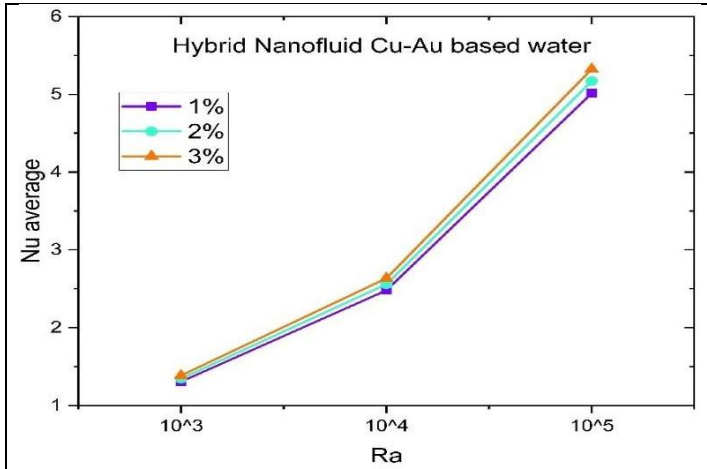


Fig. 12. Average Nusselt number as a function of Rayleigh number for the water-based Cu–Au hybrid nanofluid.

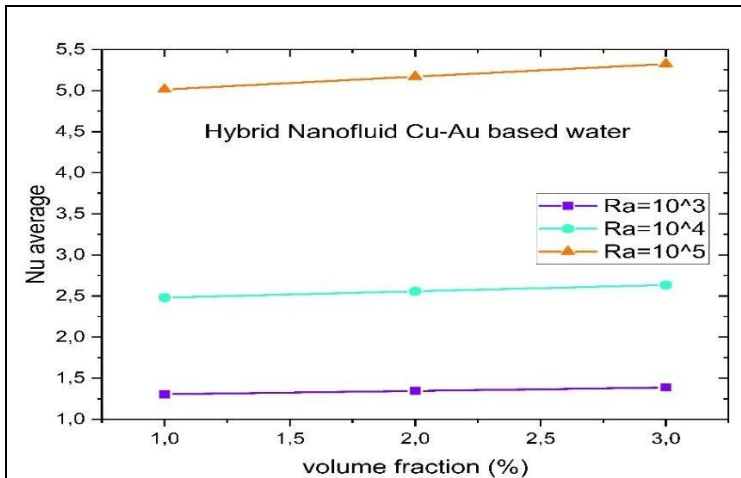


Fig. 13. Average Nusselt number as a function of volume fraction for the water-based Cu–Au hybrid nanofluid.

### 5 Conclusion

This numerical study shows that the enhancement of natural convective heat transfer in a square heated cavity filled with hybrid nanofluids mainly depends on the intensity of convection and the careful selection of the nanoparticle volume fraction. The results indicate that moderate to high Rayleigh numbers combined with volume fractions in the range of  $\phi = 2\text{-}3\%$ , provide an optimal compromise between the increase in the average Nusselt number and the viscosity-induced effects associated with nanoparticle addition, which is particularly relevant for passive thermal management systems.

The comparison between the Cu-Ag and Cu-Au hybrid nanofluids reveals that the Cu-Ag nanofluid exhibits slightly better thermal performance under all investigated conditions; however, the differences remain moderate, suggesting that the dominant mechanism is the overall enhancement of effective properties rather than the specific nature of the noble metal used.

These results corroborate the literature on hybrid nanofluids, where bimetallic combinations improve stability and thermophysical properties, while the impact of the hybrid type remains limited for similar noble metal volume fractions.

### Acknowledgements

This study was supported by the National Center for Scientific and Technical Research (CNRST) under the “PhD-Associate Scholarship Pass” program in Morocco.

### References

- [1] S. Rostami *et al.*, “A review on the control parameters of natural convection in different shaped cavities with and without nanofluid,” *Processes*, vol. 8, no. 9, p. 1011, 2020.
- [2] A. Bendaraa, M. Harchaoui, M. Elörch, W. Amlal, M. M. Charafi, and A. Hasnaoui, “Optimisation of double pipe heat exchanger using Al<sub>2</sub>O<sub>3</sub>-Cu hybrid nanofluid,” in *AIP Conference Proceedings*, AIP Publishing LLC, 2023, p. 40019.
- [3] A. You, M. Be, and I. In, “Optimisation of double pipe heat exchanger using Al<sub>2</sub>O<sub>3</sub>-Cu hybrid nanofluid □,” vol. 040019, no. June 1997, 2023.
- [4] W. Amlal, M. Harchaoui, M. Elörch, A. Bendaraa, and M. M. Charafi, “Heat transfer optimization with hybrid nanofluids under magnetic field: influence of dynamic parameters and base fluids,” *Eur. Phys. J. Plus*, vol. 140, no. 9, p. 853, 2025.
- [5] Z. Abdel-Nour *et al.*, “Magnetohydrodynamic natural convection of hybrid nanofluid in a porous enclosure: numerical analysis of the entropy generation,” *J. Therm. Anal. Calorim.*, vol. 141, no. 5, pp. 1981–1992, 2020.
- [6] M. H. M. Hashim, N. M. Arifin, A. N. M. Som, N. M. Ali, A. Ab Ghani, and S. J. Ali, “Natural convection in trapezoidal cavity containing hybrid nanofluid,” *J. Adv. Res. Micro Nano Eng.*, vol. 13, no. 1, pp. 18–30, 2023.
- [7] M. R. Hasan and M. B. Uddin, “Free Convection in a Triangular Cavity Filled with Hybrid-Nanofluid along with Sinusoidal Heat,” *Eur. J. Eng. Technol. Res.*, vol. 4, no. 12, pp. 48–52, 2019.
- [8] S. Khalatbari *et al.*, “Thermal analysis of natural convection in triangular enclosures with Al<sub>2</sub>O<sub>3</sub>- Cu/water hybrid nanofluid flow,” *J. Therm. Anal. Calorim.*, pp. 1–13, 2025.
- [9] S. Munir and Y. U. U. Bin Turabi, “Impact of heated wavy wall and hybrid nanofluid on natural convection in a triangular enclosure with embedded cold cylinder under inclined magnetic field,” *Arab. J. Sci. Eng.*, vol. 50, no. 6, pp. 4007–4020, 2025.
- [10] H. R. Ashorynejad and A. Shahriari, “MHD natural convection of hybrid nanofluid in an open wavy cavity,” *Results Phys.*, vol. 9, pp. 440–455, 2018.
- [11] M. Ghalambaz, A. Doostani, E. Izadpanahi, and A. J. Chamkha, “Conjugate natural convection flow of Ag–MgO/water hybrid nanofluid in a square cavity.,” *J. Therm. Anal. Calorim.*, vol. 139, no. 3, 2020.
- [12] F. Duan, D. Kwek, and A. Crivoi, “Viscosity affected by nanoparticle aggregation in Al<sub>2</sub>O<sub>3</sub>-water nanofluids,” *Nanoscale Res. Lett.*, vol. 6, no. 1, p. 248, 2011.

- [13] K. Khanafer, K. Vafai, and M. Lightstone, "Buoyancy-driven heat transfer enhancement in a two-dimensional enclosure utilizing nanofluids," *Int. J. Heat Mass Transf.*, vol. 46, no. 19, pp. 3639–3653, 2003.
- [14] G. de Vahl Davis, "Natural convection of air in a square cavity: a bench mark numerical solution," *Int. J. Numer. methods fluids*, vol. 3, no. 3, pp. 249–264, 1983.
- [15] A. Boualit, N. Zeraibi, T. Chergui, M. Lebbi, L. Boutina, and S. Laouar, "Natural convection investigation in square cavity filled with nanofluid using dispersion model," *Int. J. Hydrogen Energy*, vol. 42, no. 13, pp. 8611–8623, 2017.